Title

Reaction of a bridged frustrated Lewis pair with nitric oxide: a kinetics study.

Journal

Journal of the American Chemical Society, 136(1)

ISSN

0002-7863

Authors

Pereira, José Clayston Melo
Sajid, Muhammad
Kehr, Gerald
et al.

Publication Date

2014

DOI

10.1021/ja4118335

Peer reviewed

JACS
JOURNAL OF THE AMERICAN CHEMICAL SOCIETY
Article
pubs.acs.org/JACS

Reaction of a Bridged Frustrated Lewis Pair with Nitric Oxide: A Kinetics Study

José Clayston Melo Pereira,[†] Muhammad Sajid,[‡] Gerald Kehr,[‡] Ashley M. Wright,[†] Birgitta Schirmer,[‡] Zheng-Wang Qu,[§] Stefan Grimme,*[,§] Gerhard Erker,*[,‡] and Peter C. Ford*[,†]

[†]Department of Chemistry and Biochemistry, University of California at Santa Barbara, Santa Barbara, California 93106-9510, United States

[‡]Organisch-Chemisches Institut, Westfälische Wilhelms-Universität Muenster,48149 Münster, Germany

[§]Mulliken Center for Theoretical Chemistry, Institut für Physikalische und Theoretische Chemie, Universität Bonn, Beringstr. 4, D-53115 Bonn, Germany

Supporting Information

ABSTRACT: Described is a kinetics and computational study of the reaction of NO with the intramolecular bridged P/B frustrated Lewis pair (FLP) *endo*-2-(dimesitylphosphino)-*exo*-3-bis(pentafluorophenyl)boryl-norbornane to give a persistent FLP-NO aminoxyl radical. This reaction follows a second-order rate law, first-order in [FLP] and first-order in [NO], and is markedly faster in toluene than in dichloromethane. By contrast, the NO oxidation of the phosphine base 2-(dimesitylphosphino)norbornene to the corresponding phosphine oxide follows a third-order rate law, first-order in [phosphine] and second-order in [NO]. Formation of the FLP-NO radical in toluene occurs with a $\Delta H^{\ddagger}$ of 13 kcal mol^{-1}, a feature that conflicts with the computation-based conclusion that NO addition to a properly oriented B/P pair should be nearly barrierless. Since the calculations show the B/P pair in the most stable solution structure of this FLP to have an unfavorable orientation for concerted reaction, the observed barrier is rationalized in terms of the reversible formation of a [B]-NO complex intermediate followed by a slower isomerization−ring closure step to the cyclic aminoxyl radical. This combined kinetics/theoretical study for the first time provides insight into mechanistic details for the activation of a diatomic molecule by a prototypical FLP.

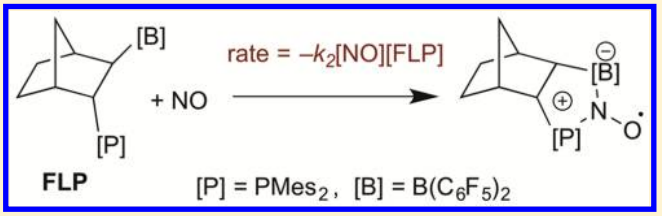

INTRODUCTION

Persistent aminoxyl radicals (also called "nitroxides") have importance as the controlling reagents in free-radical-mediated polymerization[1] and find increasing use in organic synthesis.[2] Substituted and functionalized nitroxides such as TEMPO derivatives (**1**) are mostly synthesized via amine oxidation, although an earlier example describes formation of aminoxyl radical **3** directly from nitric oxide (nitrogen monoxide, Scheme 1).[3]

Scheme 1

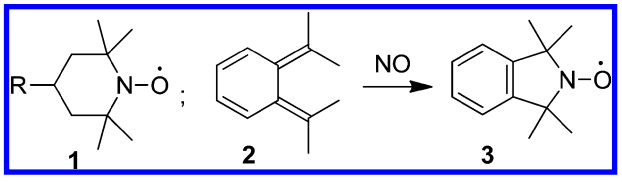

Recently, Erker, Warren, and co-workers reported another direct pathway, namely, the reaction of NO with frustrated Lewis pairs (FLPs) to give a new family of aminoxyl radicals.[4,5] FLP chemistry[6] uses steric bulk[7] to prevent Lewis acid and Lewis base pairs from forming the typically neutralizing strong adducts. The resulting FLP thus has the potential to undergo cooperative acid/base interactions with various substrates, and this leads to novel reactivities. For examples, certain FLPs can heterolytically split H_2 under mild conditions and serve as metal-free hydrogenation catalysts.[6−10] FLPs have also been shown to react with other small molecules[11−14] and to have a pronounced potential for small molecule activation.[15] In addition, intramolecular vicinal P/B FLPs such as **5**[16] and derivatives thereof[17] have been prepared by hydroboration of alkenyl phosphines and react rapidly with NO to give the corresponding persistent FLP-NO aminoxyl radicals (e.g., Scheme 2) in high yields.[4,5]

Despite the remarkable reactivities of FLPs, mechanistic investigations have largely been computational.[18] In the present study, we initiated a kinetics and computational study of the aminoxyl radical formation described in Scheme 3 to gain further insight into the quantitative reactivities of these unusual acid/base combinations. Specifically, we chose the reaction of NO with a FLP for which the sterically encumbered -$PMes_2$ and -$B(C_6F_5)_2$ groups are further discouraged from intramolecular interaction owing to the *endo*/*exo* orientations on the bridging norbornane framework.

Received: November 20, 2013
Published: December 13, 2013

   dx.doi.org/10.1021/ja4118335 | J. Am. Chem. Soc. 2014, 136, 513−519

Scheme 2

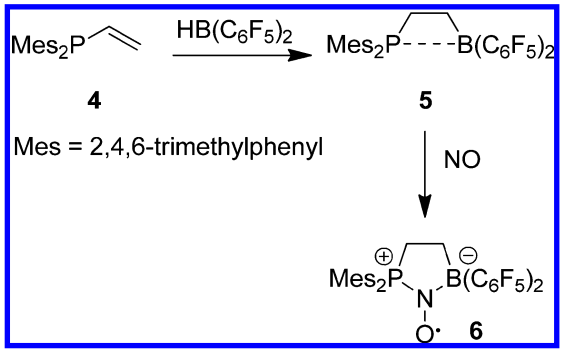

Scheme 3

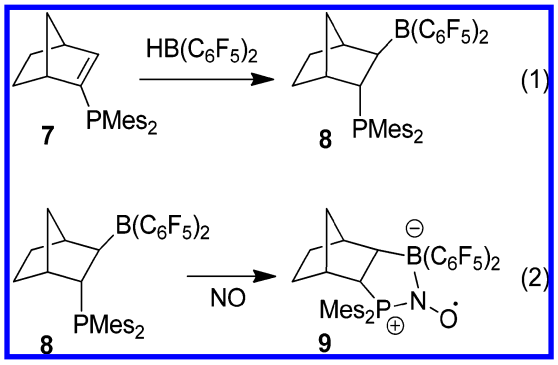

RESULTS

A. Characterization of the *in Situ* Reaction. The facile reaction of (Nor)P(Mes)$_2$ (**7**, 2-(dimesitylphosphino)-norbornene) with Piers' borane [HB(C$_6$F$_5$)$_2$)][19] gives *endo*-2-(dimesitylphosphino)-*exo*-3-bis(pentafluorophenyl)boryl-norbornane (**8**, eq 1 of Scheme 3).[5] Solutions of **8** were prepared *in situ* in the solvent of interest under strictly anaerobic and anhydrous conditions, and kinetics studies of the reaction of this FLP with NO to form the aminoxyl radical (eq 2 of Scheme 3) were monitored using temporal optical spectra changes. The NMR studies described in this section were initiated to confirm the formation of **8** under these conditions and to verify that the optical spectral changes reflect the transformations depicted in eq 2.

Typically, a small excess of HB(C$_6$F$_5$)$_2$ (1.1 equiv) was added to ensure complete hydroboration of the norbornenyl substituent of **7**. The ^{31}P NMR spectrum of **7** in dichloromethane (DCM) presents a resonance at −37.9 ppm that disappears concomitant with appearance of one at −22.0 ppm after HB(C$_6$F$_5$)$_2$ addition (Supporting Information Figure S-1), and there were no further changes for at least 16 h. Thus, with the excess HB(C$_6$F$_5$)$_2$, **7** is completely consumed, and the resulting FLP **8** is stable. The ^{1}H NMR spectra (Figure S-2) were also consistent with the hydroboration shown in eq 2. The vinyl proton (5.40 ppm) of **7** disappears, and the product spectrum displays a resonance (4.05 ppm) corresponding to the C−H adjacent to the phosphorus atom of **8**. The ^{19}F NMR spectrum of the FLP solution is shown in Figure S-3.

The reaction of NO with the FLP **8** prepared *in situ* in deuterio-DCM led to the changes in the ^{31}P, ^{19}F, and ^{1}H NMR spectra shown in Figures S-4 to S-6. The spectra for the aminoxyl radical product **9** are subject to paramagnetic broadening and were not observed. Nevertheless, several key features emerge. First, although NO is known to oxidize free phosphines[20−22] (for example, eq 3 in Scheme 4), the ^{31}P NMR spectrum displayed *no new resonances* ascribable to the

Scheme 4

phosphine oxide (Nor)P(O)Mes$_2$. Second, the ^{1}H NMR spectra displayed markedly decreased intensities of the resonances assigned to **8** relative to that at 5.32 ppm ascribed to the proton impurity in the DCM-d_2 as expected for the consumption of the FLP **8** to give **9.** Third, the decreased intensities of the ^{19}F NMR resonances for **8** compared to those for the excess free HB(C$_6$F$_5$)$_2$ (Figure S-6) indicate that the FLP was consumed by reaction with NO.

Aminoxyl radicals oxidize 1,4-cyclohexadiene (CHD) to benzene,[2,4,5] and this reaction was used to confirm the *in situ* formation of **9** (eq 2). A deuterio-DCM solution of **8** was prepared by adding less than a stoichiometric amount of HB(C$_6$F$_5$) to (Nor)P(Mes)$_2$ (5 μmol in 1 mL solution). The ^{31}P NMR spectrum showed resonances for **8** (singlet at −22.0 ppm) and the excess **7** (singlet at −37.9 ppm) in an integrated ratio of 1.0 to 0.5 (Figure S-7). After adding NO (4×) and CHD (10×), the ^{31}P NMR spectrum showed complete disappearance of the resonance at −22.0 ppm and the appearance of a sharp singlet at 41.0 ppm attributed to the diamagnetic product **10**. The ^{31}P NMR resonance at −37.9 ppm for the excess **7** remained unchanged (Figure S-8), and the integrated ratio of the respective singlets in the product spectrum was 1.0 to 0.5. Thus, the hydrogen abstraction reaction illustrated in Scheme 5 is occurring readily without significant depletion of the excess (Nor)P(Mes)$_2$ present.

Scheme 5

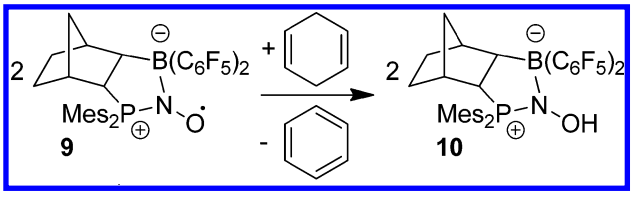

Similarly, ^{1}H NMR spectra showed that resonances at 6.74 and 6.51 ppm ascribed to the mesityl groups of **8** disappeared upon addition of NO. Upon addition of CHD, resonances at 7.08, 6.95, 6.90, 6.80, 6.77, and 4.66 ppm corresponding to **10** and the excess **7** were observed (Figure S-8). Also seen was a new singlet at 7.35 ppm attributed to benzene. By using the methyl protons of added [Si(CH$_3$)$_3$]$_2$O as an internal standard, the calculated amounts of **10** and benzene formed were 3.0 μmol and 1.74 μmol, respectively, in a ratio approximating the 2 to 1 stoichiometry of Scheme 5. Notably, the initial solution contained 5.0 μmol of **7** but only two-thirds of this was converted to **8** (3.3 μmol) according to Figure S-7, so the amount of benzene formed corresponds well to that expected.

B. Kinetics Studies. *Reaction between NO and 7.* The progress of this reaction (eq 4) was followed by recording the

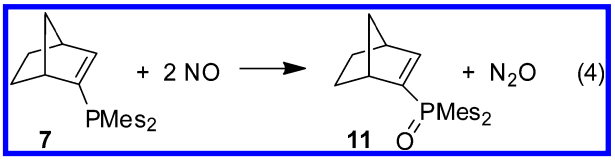

dx.doi.org/10.1021/ja4118335 | J. Am. Chem. Soc. 2014, 136, 513−519

temporal changes in the near-UV spectrum. Earlier studies have shown that triaryl phosphines are oxidized by NO (eq 3) via a rate law that is first-order in $[R_3P]$ and second-order in [NO].[20−22] Although the reaction of FLP with NO gives a different product, it was deemed important to establish a baseline for the expected reactivity of NO with the phosphine component under these conditions. To this end, the kinetics for the NO oxidation of free (Nor)P(Mes)$_2$ (eq 4) were studied in DCM. The conditions were "pseudo-first-order", meaning that the NO present in the system was in substantial stoichiometric excess, and the effective change in [NO] was small during any kinetics experiment. The reaction vessel was a closed spectrophotometer cell adapted for solution preparation using Schlenk vacuum line techniques (Figure S-9). In such a system, the bulk of the NO resides in the headspace during the course of the experiment, owing to the large partition coefficient between the liquid and gas phases and the substantially larger volume of the gas phase. Therefore, the solution phase [NO] was maintained at a near constant level by shaking the reaction vessel between spectral measurements.

Figure 1 shows the temporal absorption changes at 292 nm for a typical kinetics experiment for the reaction of NO with **7**

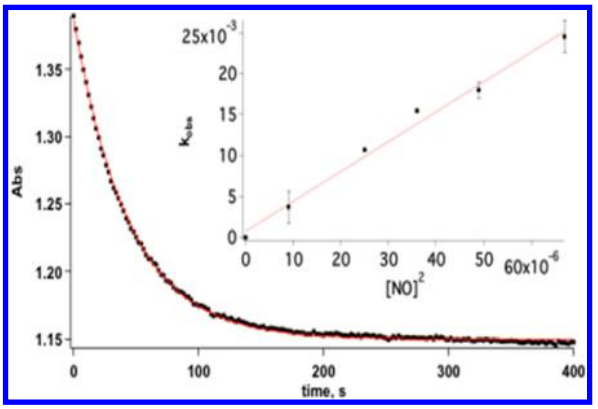

Figure 1. Temporal absorption changes at 292 nm for the reaction of NO (8.2 mM) with (Nor)P(Mes$_2$) (**7**) (50 μM) in DCM. The solid curve (red) represents the fit to an exponential function with k_{obs} = 2.3 × 10^{-2} s^{-1}. Inset: plot of k_{obs} vs $[NO]^2$ for the NO oxidation of **7** in DCM. The slope is the third-order rate constant k_3 = (3.6 ± 0.2) × 10^2 M^{-2} s^{-1} (293 K).

in DCM. The curve can be fit well to an exponential decay function (k_{obs} = (2.3 ± 0.1) × 10^{-2} s^{-1}), indicating the rate to be first-order in the limiting reagent **7**. A plot of the k_{obs} values obtained at different NO concentrations against $[NO]^2$ proved to be linear (Figure 1, inset), thus confirming the third-order rate law (eq 5) for this substrate. The overall third-order rate constant (k_3) determined in this manner is (3.6 ± 0.2) × 10^2 M^{-2} s^{-1}, which is similar in magnitude to the k_3 values determined in previous studies for triaryl phosphines in organic solvents.[20] For example, the k_3 determined here for **7** in DCM is about a factor of 3 smaller than that reported for the NO oxidation of Ph_3P in chloroform under analogous conditions.[20]

$$\frac{d[\mathbf{7}]}{dt} = -k_3[NO]^2[\mathbf{7}] \quad (5)$$

Reaction between NO and FLP ***8***. Absorbance changes at 280 nm (Figure 2) were used to follow the reaction of NO with **8** to form the aminoxyl radical **9** (eq 2) in several solvents. Again, under pseudo-first-order conditions (excess NO) the

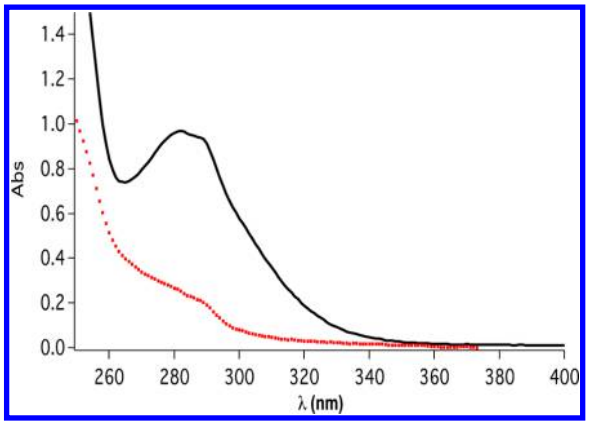

Figure 2. Spectra of the FLP **8** (200 μM) in DCM solution (black solid line) and of the reaction products after addition of NO (red dashed line).

temporal optical density decreases followed exponential decay (Figure S-10) indicating that the reaction is first-order in [**8**]. Unlike the reaction with the free phosphine **7**, these reactions were first-order in the NO concentration as evidenced by linear plots of these k_{obs} values versus [NO]. Figure 3 illustrates such

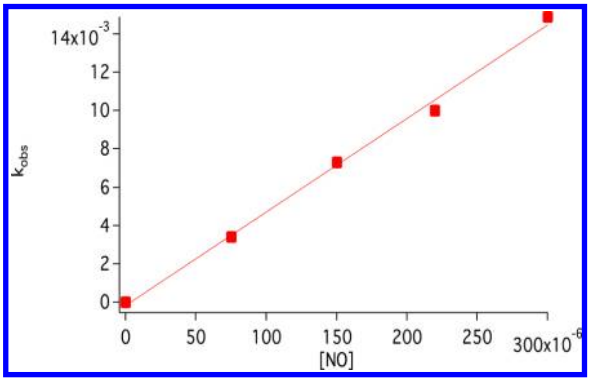

Figure 3. Plot of k_{obs} vs [NO] for the reaction of NO with the FLP **8** (initial concentration 25 μM) in toluene. The slope of the line (k_2) is 48.9 ± 1.8 M^{-1} s^{-1} (293 K).

a plot for the reaction of **8** with NO in 293 K toluene. This rate law (eq 6) proved valid in cyclohexane and DCM (Figure S-11) solutions as well. Furthermore, the rate constants k_2 are solvent-dependent, the values being 0.51 ± 0.05, 26 ± 0.6, and 48.9 ± 1.8 M^{-1} s^{-1} in DCM, cyclohexane, and toluene, respectively, at 293 K. Notably, this pattern is opposite to that seen for the third-order rates of triarylphosphine oxidations by NO (eq 3), which is favored by more polar solvents.[20]

$$\frac{d[\mathbf{8}]}{dt} = -k_2[NO][\mathbf{8}] \quad (6)$$

The much lower k_2 value for the reaction in DCM led us to examine briefly the rates in mixed toluene/DCM solutions. Table 1 summarizes the k_{obs} values determined from exponential decays as in Figure S-10 with several solvent mixtures for [NO] = 300 μM and T = 293 K. Remarkably, the presence of only 1% DCM suppressed the rate of adduct formation by a factor of 2, while 10% DCM suppressed the rate by a factor of 7. These data suggest some specific inhibition of the reaction by DCM.

dx.doi.org/10.1021/ja4118335 | J. Am. Chem. Soc. 2014, 136, 513−519

Table 1. k_{obs} Values for the Reaction between 8 and NO in Different Dichloromethane/Toluene Mixtures[a]

DCM/toluene (v/v)	k_{obs} (s^{-1}) × 10^4
100/0	1.5 ± 0.15
10/90	21 ± 1
1/99	77 ± 4
0/100	150 ± 6

[a]Conditions: [**8**] = 25 μM, [NO] = 300 μM. T: 293 K.

The temperature dependence of the rates of the NO reaction with **8** were evaluated in toluene solution over the range 15−30 °C. Plots of k_{obs} versus [NO] were linear at all temperatures (Figure S-12), and the resulting k_2 values are summarized in Table 2. An Eyring plot of these data proved to be linear

Table 2. Temperature Effects on the Second Order Rate Constants for the Reaction between 8 and NO in Toluene

T (K)	k_2 (M^{-1} s^{-1})
288	29.8 ± 3.7
293	48.9 ± 1.8
298	65.1 ± 2.9
303	98.6 ± 9.1

Conditions: [FLP] = 25 μM, [NO] = 75−300 μM.

(Figure S-13), and from this the activation parameters $\Delta H^{\ddagger}$ and $\Delta S^{\ddagger}$ for the reaction in toluene were determined to be 13.1 ± 0.3 kcal mol^{-1} and −6.1 ± 1 cal mol^{-1} K^{-1}, respectively. A comparable $\Delta H^{\ddagger}$ (11 ± 2 kcal mol^{-1}) and a somewhat more negative $\Delta S^{\ddagger}$ (−13 ± 5 cal mol^{-1} K^{-1}) were obtained for the reaction in cyclohexane, but experimental uncertainties were larger.

DFT ANALYSIS AND DISCUSSION

The NMR data described have confirmed that the reaction of the intramolecular frustrated Lewis pair **8** with NO to give the aminoxyl radical **9** occurs readily without significant by-products. This is the case even in the presence of modest quantities of the free phosphine (Nor)P(Mes)$_2$ or of the free borane HB(C$_6$F$_5$)$_2$. Very little, if any, of the phosphine oxides were seen, suggesting that, under the conditions of the NMR experiments, the known[20−22] oxidation of phosphines by NO is too slow to play a significant role. This conclusion was also drawn from the kinetic studies, which showed that the reaction of **7** with NO is a slow, third-order process (second-order in [NO]), while that of **8** with NO displays second-order kinetics (first-order in [NO]). Furthermore, the solvent effects are different, with the phosphine oxidation being faster in chloroform than in toluene,[20] while aminoxyl radical formation is slower in DCM than in toluene.

These observations point to the essential participation of the boron Lewis acid in the reaction of **8** with NO. In this context, we can formulate three limiting cases that may account for this situation (see Scheme 6). Nitric oxide might first add (potentially reversibly) to the phosphine to give the [P]-NO intermediate **12** (pathway a) that is then trapped intramolecularly by the borane Lewis acid to give **9**. Alternatively, NO might add to the borane to give the [B]-NO intermediate **13** (pathway b), which then might be trapped by the internal phosphine nucleophile. A third pathway (c) would be the concerted P/B-NO addition to give the FLP-NO aminoxyl radical **9** in a single step.

Scheme 6

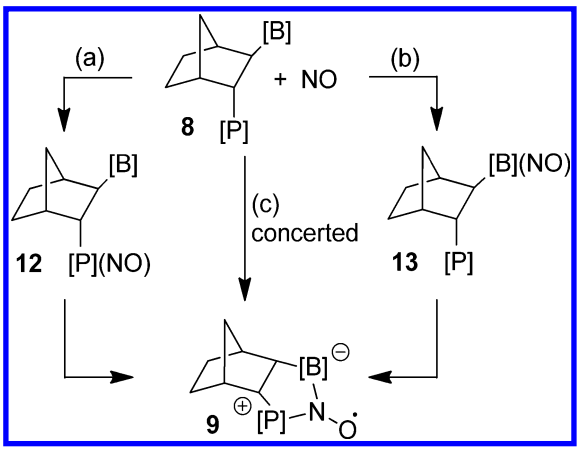

The relatively slow formation of **9** in DCM is not a simple general solvent effect, since as little as 1% DCM (∼0.16 M) in toluene/DCM mixtures led to ∼2-fold suppression of the rate relative to that in pure toluene. This suggests a very specific molecular interaction of CH_2Cl_2 with the FLP in a manner that reduces the reactivity of **8** toward NO, although it is not obvious what this interaction might be. According to the donor/acceptor parameters defined by Gutmann,[23] DCM is a weak donor (although stronger than a hydrocarbon) but a reasonably strong acceptor. Thus, it may well be that a cooperative intramolecular interaction of the Lewis acid and Lewis base in **8** with CH_2Cl_2 gives a weak complex for which the reactivity with NO is suppressed. Given the extent to which the rate is decreased at 1% CH_2Cl_2, one may estimate the equilibrium constant for this complex formation to be ∼6 M^{-1} in toluene solution. This corresponds to a free energy change of about 1 kcal mol^{-1}, which is difficult to be checked with DFT calculations. Since the observed solvent effects for the oxidation of phosphines by NO are consistent with the involvement of polar [P]-NO intermediates, the reversed solvent effects observed for the reaction between **8** and NO could indicate the involvement of less polar intermediates such as the [B]-NO intermediate **13**.

We have tried to evaluate the alternatives indicated in Scheme 6 with the aid of DFT computations (for details see the Supporting Information).[24] The free energies from TPSS-D3/def2-TZVP calculations plus thermal and solvent corrections in toluene will be used in our discussion unless explicitly specified otherwise.

We first investigated the activation barrier of a direct reaction of the FLP **8** with NO to give the FLP-NO radical **9**. By removing the NO moiety from the X-ray structure of **9**, the reactive FLP conformer **8-X** is obtained after DFT geometry optimization. In this conformer, both the phosphinyl and the boryl substituents are found in the *right*-handed propeller arrangement, with the P-atom electron lone pair pointing toward the B-atom empty *p*-orbital. Due to such cooperative Lewis acid/base interactions at an appropriate B−P distance of about 3.4 Å in **8-X**, our calculations revealed a practically barrier-free, concerted NO-addition to give **9** (see Figure 4).

This result appears quite reasonable upon an inspection of the (experimental) X-ray structure of **9** and the computed structure **8-X**. An overlay of the two structures indicates a remarkable structural similarity (see Figure 5). The incoming NO can simultaneously accept electron density from the P-

dx.doi.org/10.1021/ja4118335 | J. Am. Chem. Soc. 2014, 136, 513−519

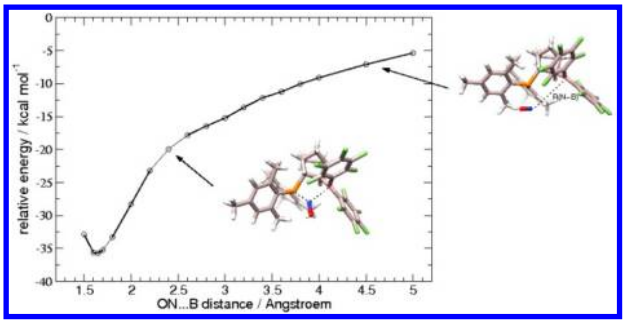

Figure 4. DFT calculated gas phase reaction energy profile of the practically barrier-free concerted FLP [**8-X**] + NO addition reaction.

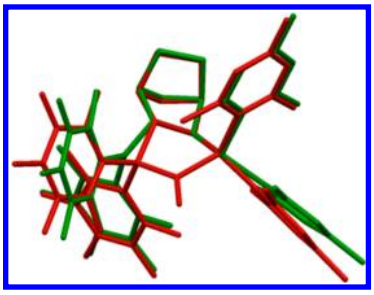

Figure 5. Overlay of the DFT-optimized FLP conformer **8-X** (in green) and the X-ray structure of **9** (in red).

centered lone pair into partially filled π^*-orbitals and back-donate σ electron lone pairs into the B-centered empty *p*-orbital. No appreciable enthalpy barrier $\Delta H^{\ddagger}$ could be expected for such a concerted reaction step. Obviously, the suggested reactivity of reactive conformer **8-X** is in striking disagreement with the clearly observed activation barrier for the reaction of **8** with NO in solution.

However, **8-X** is only a local conformational FLP minimum. The global minimum (**8-S**) calculated by DFT is very similar to the structure of the FLP **8** found in the crystal.[5] It is 5.1 kcal mol^{-1} lower in free energy than the reactive local minimum conformer **8-X**. Conformer **8-S** is converted to **8-X** by a rotational mechanism with a DFT calculated activation energy ($\Delta G^{\ddagger}$) of 10.9 kcal mol^{-1}. Actually, we have experimentally observed by dynamic NMR spectroscopy that the two related mesityl rotational processes around the P-aryl vectors in **8** have barriers of $\Delta G^{\ddagger}_{rot}$(213K) = 9.8 kcal mol^{-1} and $\Delta G^{\ddagger}_{rot}$(243K) = 11.4 kcal mol^{-1}, respectively, (for details see the Supporting Information). The DFT calculation has also revealed a second possible process for the **8-S** to **8-X** conversion by a pathway involving stereochemical inversion at phosphorus, but that is markedly higher in energy (see Figure 6).

Although the alleged pathway of the formation of **9** from **8** and NO by the **8-S** to **8-X** conformational conversion followed by a concerted NO addition seems attractive, it is not in accord with the result of our kinetic study. In that pathway the first step involving phosphinyl conformational rearrangement would be rate-limiting and the overall reaction should consequently be zero-order in [NO]. However, this appears inconsistent with the experimentally observed first-order kinetics of the reaction of **8** with NO giving **9**.

The alternative mechanisms start from NO-addition at either the electron-rich P-center or the electron-deficient B-center within **8-S**, followed by a ring-closure step to form the final product **9**. The NO addition leads to the weak complexes **12** and **13**, respectively (see Figure 7). Such complexes are so weak

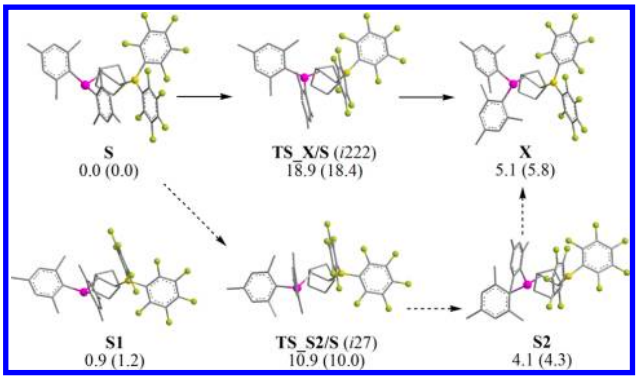

Figure 6. DFT calculated low-lying FLP **8** conformers and conformational conversions in solution. For each structure, the phosphanyl, the boryl, and the norbornane bridge are always put on the left, the right, and the bottom, respectively, and the relative free energies (in toluene at 298 K, enthalpies in parentheses) are shown in kcal mol^{-1}.

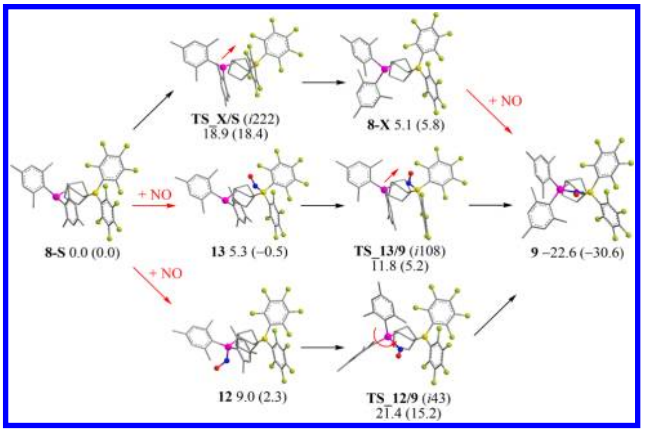

Figure 7. DFT calculated free energy pathways (in toluene at 298 K in kcal mol^{-1}, ΔH in parentheses) for the FLP **8** + NO reaction.

that they become almost unbound after thermal and solvation corrections and even repulsive by the single-point PW6B95-D3 hybrid functional. Due to the relatively complicated electronic configuration of the NO radical (i.e., a single electron in a degenerate π^* orbital) and the tendency of approximate density functionals to overdelocalize the spin, there are some uncertainties for the computed NO-binding energies of these weak complexes. Other "isomerization" steps and the overall mechanistic picture are not affected significantly by this problem. Our DFT calculations consistently suggest that the P···N complex **12** is more polar but less stable than the B···N complex **13**.

Due to some steric clash between the bulky phosphanyl group and the norbornane bridge, ring closure through a large-amplitude phosphinyl rotation (**TS_12/9**) within the P-centered complex **12** is prevented by a barrier $\Delta G^{\ddagger}$ of 12.4 kcal mol^{-1}. On the other hand, ring closure through the NO-aided phosphinyl inversion (**TS_13/9**) within the B-centered complex **13** is much easier with lower barrier $\Delta G^{\ddagger}$ of only 6.5 kcal mol^{-1}, leading to the same five-membered-ring product **9**. As expected, both conversion barriers become somewhat larger at the higher PW6B95-D3 level of theory (see Table 3).

The suggested preferred NO-addition mechanism through the B-centered intermediate **13** for the FLP **8** + NO reaction is further supported by comparison with the experimental observations. First, the overall barrier $\Delta G^{\ddagger}$ is computed to be

dx.doi.org/10.1021/ja4118335 | J. Am. Chem. Soc. 2014, 136, 513−519

Table 3. Comparison of DFT Computed Reaction Free Energies and Reaction Barriers for Two Density Functionals (298 K, in Toluene in kcal/mol)

	TPSS-D3/def2-TZVP	PW6B95-D3/def2-TZVP
	ΔG	
8-S + NO → **13**	5.3	12.8
8-S + NO → **12**	9.0	14.0
8-S + NO → **9**	−22.6	−21.8
	$\Delta G^{\ddagger}$	
13 → **9**	6.5	7.0
12 → **9**	12.4	15.7
8-S + NO → **9**	11.8	19.7

11.8 kcal mol^{-1} at the TPSS-D3 level, which is only 3.1 kcal mol^{-1} lower than the experimental value of 14.9 ± 0.3 kcal mol^{-1} in toluene. At the PW6B95-D3 hybrid level the computed barrier is as expected significantly higher, and the two theoretical results bracket the experimental value. The measured $\Delta S^{\ddagger}$ of −6.1 ± 1 cal mol^{-1} K^{-1} (calcd: −2.6 ± 1 cal mol^{-1} K^{-1} for **13** to **TS 13/9**) is consistent with the involvement of a weak [B]-NO complex as intermediate involved in the rate-determining step, which otherwise should be much more negative around −20 cal mol^{-1} K^{-1} for single-step NO-capture reaction (calcd: −22.3 cal mol^{-1} K^{-1} for **8S** to **TS 13/9**). Second, the suggested kinetic model with reversible NO and FLP complex formation followed by a slower ring-closure step is consistent with the observed first-order kinetics in [NO] concentration. Finally, the preferred B-centered intermediate **13** is less polar than the P-centered intermediate **12** (computed dipole moment of 4.8 vs 6.2 D), which is at least partially consistent with the observed solvent effects.

In summary, our kinetic analysis points to the participation of both the phosphine Lewis base and the borane Lewis acid in determining the rate of the FLP **8** + NO reaction. Our experimental observations and DFT calculations suggest that the reaction starts from the internally stabilized conformer **8-S** in solution. The NO molecule is added first through an electron lone-pair to the electron-deficient boron center to aid the subsequent inversion at the P-center to give the persistent FLP-NO radical **9**. The P/B FLP + NO addition observed here is only formally reminiscent of a cheletropic reaction (similar to the NO reaction with the *o*-quinodimethane derivative **2** depicted in Scheme 1). Instead it appears to follow a two-step pathway consisting of reversible NO addition to the borane Lewis acid followed by rate-determining intramolecular trapping of the [B]-NO intermediate by the adjacent phosphane Lewis base. We also note that the facile NO binding by the cooperative action of the B-acceptor and the P-donor of the FLP **8** has some analogy to the bonding/back bonding of NO to a transition metal,[25] although in this case the donor and the acceptor functions are derived from different atoms within the bifunctional vicinal FLP.[26]

EXPERIMENTAL SECTION

Nitric Oxide Solutions and Reactions. The NO was transferred from a commercial tank (Praxair) via stainless steel lines. The NO was purified of NO_2 and N_2O_3 by passing through a stainless steel column containing Ascarite II.[27] A deoxygenated flask, equipped with an injection port, was pressurized to 760 Torr with NO. A small volume of NO was removed from this flask with a previously deoxygenated gastight syringe and added to the Schlenk cuvette (Figure S-9) containing the FLP **8** that had been prepared *in situ* (see below) in 3.0 mL of the solvent (this part of the procedure was carried out in a glovebox.). The Schlenk quartz cuvettes used for reaction studies (Figure S-9) have a known volume 47 mL, and concentration in the solution was calculated from this volume and the partition coefficient between the liquid and gas phases. The kinetics of the reaction were followed by recording the optical spectrum every 20 s. After each spectral measurement, the reaction flask was vigorously shaken to maintain the equilibrium between the liquid and gas phases. This procedure was necessary because the volume of the gas phase (47 mL) was much larger than that of the solution phase (3.0 mL) and the concentration of NO in the solution phase is lower than in gas phase. Thus, the total amount of NO present in the system (675−900 pmol) was in significant excess to the amount of FLP (75 pmol). Therefore, the NO concentration remained approximately constant (pseudo-first-order conditions) throughout any individual kinetics run.

The solubility of NO in toluene and cyclohexane was obtained directly from the literature, extrapolating where necessary.[28−30] The solubility in DCM was assumed to parallel that of O_2, which is known for each of the solvents used here.[28,29] Therefore, the Ostwald coefficients for NO were estimated from the product of the known Ostwald coefficient for O_2 in that solvent, $L(O_2)$, times the average (1.068) of the Ostwald coefficient ratios for two related solvents in which both are known, toluene ($L(NO)/L(O_2)$) = 1.094) and carbon tetrachloride (1.043).[20−22] This led to $L(NO)$ estimates of 0.27 for DCM.

Instrumental Methods. Optical absorbance measurements were recorded using a Shimadzu dual beam UV-2401 PC Spectrophotometer in 1.00-cm path-length quartz cells. For all kinetics studies, the spectrometer cell compartment was thermostatted to appropriate temperature (288, 293, 298, or 303 K). NMR spectra were recorded on a Varian UNITY INOVA 400 or Varian UNITY INOVA 500 spectrometer. The ^1H NMR spectra were referenced to external $SiMe_4$ using the residual protio solvent peaks as an internal standard. The $^{19}F\{^1H\}$ NMR spectra were referenced to external $CFCl_3$, and $^{31}P\{^1H\}$ NMR spectra were referenced to external 85% phosphoric acid

Preparation of Solutions for Kinetics. The *in situ* synthesis of the FLP **8**, which involves air- and moisture-sensitive compounds, was carried out in a glovebox in dry solvent under an atmosphere of argon. A solution of $(Nor)P(Mes)_2$ (2.7 mg, 2.5 mM) and $HB(C_6F_5)_2$ (2.7 mg, 2.6 mM) in 3 mL of the solvent of interest was stirred for 15 min at room temperature to produce **8**. A small volume (30 μL) of the resulting stock solution was transferred from the flask with a deaerated syringe and added to the Schlenk cell containing 3 mL of dry toluene, DCM, or cyclohexane to give a final concentration of 25 μM.

ASSOCIATED CONTENT

Supporting Information

^1H, ^{31}P, and ^{19}F NMR spectra of reactants and products of NO reactions with FLP **8** and phosphine **7**, kinetics data, reaction cell used to measure temporal absorbances during the reactions, and DFT calculation details. This material is available free of charge via the Internet at http://pubs.acs.org.

AUTHOR INFORMATION

Corresponding Authors

erker@uni-muenster.de
ford@chem.ucsb.edu
grimme@thch.uni-bonn.de

Notes

The authors declare no competing financial interest.

ACKNOWLEDGMENTS

This work was supported by grants to P.C.F. from U.S. National Science Foundation (CHE-1058794) and to G.E. from the European Research Council. S.G. and Z.W.Q. acknowledge support by the DFG in the framework of the SFB 813 ("Chemistry at Spin-Centers"). J.C.M.P. thanks

Coordenação de Aperfeiçoamento de Pessoal de Nível Superior.

REFERENCES

(1) (a) Hawker, C. J.; Bosman, A. W.; Harth, E. *Chem. Rev.* **2001**, *101*, 3661. (b) Studer, A. *Chem. Soc. Rev.* **2004**, *33*, 267. (c) Studer, A.; Schulte, T. *Chem. Rec.* **2005**, *5*, 27. (d) Brinks, M. K.; Studer, A. *Macromol. Rapid Commun.* **2009**, *30*, 1043. (e) Sciannamea, V.; Jérôme, R.; Detremleur, C. *Chem. Rev.* **2008**, *108*, 1104 and references therein.

(2) Tebben, L.; Studer, A. *Angew. Chem., Int. Ed.* **2011**, *50*, 5034.

(3) Korth, H. G.; Ingold, K. U.; Sustmann, R.; de Groot, H.; Sies, H. *Angew. Chem., Int. Ed.* **1992**, *31*, 891.

(4) (a) Cardenas, A. J. P.; Culotta, B. J.; Warren, T. H.; Grimme, S.; Stute, A.; Fröhlich, R.; Kehr, G.; Erker, G. *Angew. Chem., Int. Ed.* **2011**, *50*, 7567. (b) Sajid, M.; Stute, A.; Cardenas, A. J. P.; Culotta, B. J.; Hepperle, J. A. M.; Warren, T. H.; Schirmer, B.; Grimme, S.; Studer, A.; Daniliuc, C. G.; Fröhlich, R.; Petersen, J. L.; Kehr, G.; Erker, G. *J. Am. Chem. Soc.* **2012**, *134*, 10156. (c) Warren, T. H.; Erker, G. *Top. Curr. Chem* . **2013**, *334*, 219.

(5) Sajid, M.; Kehr, G.; Wiegand, T.; Cardenas, A. J. P.; Schwickert, C.; Pöttgen, R.; Eckert, H.; Warren, T. H.; Fröhlich, R.; Daniliuc, C. G.; Erker, G. *J. Am. Chem. Soc.* **2013**, *135*, 8882.

(6) (a) Stephan, D. W.; Erker, G. *Angew. Chem., Int. Ed.* **2010**, *49*, 46. (b) Erker, G.; Stephan, D. W. *Frustrated Lewis Pairs I*; Springer-Verlag: Berlin, Heidelberg, 2013; Topics in Current Chemistry Vol. *332*. (c) Erker, G.; Stephan, D. W. *Frustrated Lewis Pairs II*; Springer-Verlag: Berlin, Heidelberg, 2013, Topics in Current Chemistry Vol. *334*.

(7) (a) Welch, G. C.; Juan, R. R. S.; Masuda, J. D.; Stephan, D. W. *Science* **2006**, *314*, 1124. (b) Welch, G. C.; Stephan, D. W. *J. Am. Chem. Soc.* **2007**, *129*, 1880.

(8) (a) For an electronic alternative see, e.g.: Stute, A.; Kehr, G.; Fröhlich, R.; Erker, G. *Chem. Commun.* **2011**, *47*, 4288. (b) Rosorius, C.; Kehr, G.; Fröhlich, R.; Grimme, S.; Erker, G. *Organometallics* **2011**, *30*, 4211.

(9) (a) Chernichenko, K.; Madarász, Á.; Pápai, I.; Nieger, M.; Leskelä, M.; Repo, T. *Nat. Chem.* **2013**, *5*, 718−723. (b) Greb, L.; Oña-Burgos, P.; Schirmer, B.; Grimme, S.; Stephan, D. W.; Paradies, J. *Angew. Chem., Int. Ed.* **2012**, *51*, 10164. (c) Xu, B.-H.; Kehr, G.; Fröhlich, R.; Wibbeling, B.; Schirmer, B.; Grimme, S.; Erker, G. *Angew. Chem., Int. Ed.* **2011**, *50*, 7183. (d) Reddy, J. S.; Xu, B.-H.; Mahdi, T.; Fröhlich, R.; Kehr, G.; Stephan, D. W.; Erker, G. *Organometallics* **2012**, *31*, 5638. (e) Erker, G.; Stephan, D. W. *Top. Curr. Chem.* **2013**, *332*, 85.

(10) (a) Mömming, C. M.; Frömel, S.; Kehr, G.; Fröhlich, R.; Grimme, S.; Erker, G. *J. Am. Chem. Soc.* **2009**, *131*, 12280. (b) Voss, T.; Sortais, J.-B.; Fröhlich, R.; Kehr, G.; Erker, G. *Organometallics* **2011**, *30*, 584. (c) Chen, C.; Fröhlich, R.; Kehr, G.; Erker, G. *Chem. Commun.* **2010**, *46*, 3580. (d) Voss, T.; Chen, C.; Kehr, G.; Nauha, E.; Erker, G.; Stephan, D. W. *Chem.—Eur. J.* **2010**, *16*, 3005. (e) Chen, C.; Eweiner, F.; Wibbeling, B.; Fröhlich, R.; Senda, S.; Ohki, Y.; Tatsumi, K.; Grimme, S.; Kehr, G.; Erker, G. *Chem. Asian J.* **2010**, 4711. (f) Mömming, C. M.; Kehr, G.; Wibbeling, B.; Fröhlich, R.; Schirmer, B.; Grimme, S.; Erker, G. *Angew. Chem., Int. Ed.* **2010**, *49*, 2414. (g) Mömming, C. M.; Kehr, G.; Fröhlich, R.; Erker, G. *Chem. Commun.* **2011**, *47*, 2006.

(11) Mömming, C. M.; Kehr, G.; Fröhlich, R.; Erker, G. *Dalton Trans.* **2010**, *39*, 7556.

(12) (a) Mömming, C. M.; Otten, E.; Kehr, G.; Fröhlich, R.; Grimme, S.; Stephan, D. W.; Erker, G. *Angew. Chem., Int. Ed.* **2009**, *48*, 6643. (b) Peuser, I.; Neu, R. C.; Zhao, X.; Ulrich, M.; Schirmer, B.; Tannert, J. A.; Kehr, G.; Fröhlich, R.; Grimme, S.; Erker, G.; Stephan, D. W. *Chem.—Eur. J.* **2011**, *17*, 9640.

(13) Sajid, M.; Klose, A.; Birkmann, B.; Liang, L.; Schirmer, B.; Wiegand, T.; Eckert, H.; Lough, A. J.; Fröhlich, R.; Daniliuc, C. G.; Grimme, S.; Stephan, D. W.; Kehr, G.; Erker, G. *Chem. Sci.* **2013**, *4*, 213.

(14) Otten, E.; Neu, R. C.; Stephan, D. W. *J. Am. Chem. Soc.* **2009**, *131*, 9918.

(15) Sajid, M.; Elmer, L.-M.; Rosorius, C.; Daniliuc, C. G.; Grimme, S.; Kehr, G.; Erker, G. *Angew. Chem. Int., Ed.* **2013**, *52*, 2243.

(16) Spies, P.; Erker, G.; Kehr, G.; Fröhlich, R.; Grimme, S.; Stephan, D. W. *Chem. Commun.* **2007**, 5072.

(17) Axenov, K.; Mömming, C. M.; Kehr, G.; Fröhlich, R.; Erker, G. *Chem.—Eur. J.* **2010**, *17*, 14069.

(18) (a) Zhao, L.; Li, H.; Lu, G.; Wang, Z.-X. *Dalton Trans.* **2010**, *39*, 4038. (b) Dang, L. X.; Schenter, G. K.; Chang, T.-M.; Kathmann, S. M.; Autrey, T. *J. Phys. Chem. Let.* **2012**, *3*, 3312. (c) Rokob, T. A.; Bakó, I.; Stirling, A.; Hamza, A.; Papai, I. *J. Am. Chem. Soc.* **2013**, *135*, 4425.

(19) (a) Parks, D. J.; Spence, R. E. v H.; Piers, W. *Angew. Chem., Int. Ed.* **1995**, *34*, 809. (b) Spence, R. E. v H.; Parks, D. J.; Piers, W. E.; MacDonald, M.-A.; Zaworotko, M. J.; Rettig, S. J. *Angew. Chem., Int. Ed.* **1995**, *34*, 1230. (c) Piers, W. E.; Chivers, T. *Chem. Soc. Rev.* **1997**, *26*, 345. (d) Spence, R. E. v H.; Piers, W. E.; Sun, Y.; Parvez, M.; MacGillivray, R.; Zaworotko, M. J. *Organometallics* **1998**, *17*, 2459.

(20) Lim, M. D.; Lorkovic, I. L.; Ford, P. C. *Inorg. Chem.* **2002**, *41*, 1026.

(21) Bakac, A.; Schouten, M.; Johnson, A.; Song, W.; Pestovsky, O.; Szajna-Fuller, E. *Inorg. Chem.* **2009**, *48*, 6979.

(22) Heinecke, J. L.; Khin, C.; Pereira, J. C. M.; Suarez, S. A.; Iretskii, A. V.; Doctorovich, F.; Ford, P. C. *J. Am. Chem. Soc.* **2013**, *135*, 4007.

(23) Gutmann, V. *The Donor-Acceptor Approach to Molecular Interaction*; Plenum: New York, 1978.

(24) (a) Grimme, S. *J. Chem. Phys.* **2006**, *124*, 034108. (b) Grimme, S.; Antony, J.; Ehrlich, S.; Krieg, H. *J. Chem. Phys.* **2010**, *132*, 154104. (c) Grimme, S.; Ehrlich, S.; Goerigk, L. *J. Comput. Chem.* **2011**, *32*, 1456. (d) Weigend, F.; Ahlrichs, R. *Phys. Chem. Chem. Phys.* **2005**, *7*, 3297. (e) Grimme, S. *Chem.—Eur. J.* **2012**, *18*, 9955. (f) Eckert, F., Klamt, A. *COSMOtherm*, Version C2.1, Release 01.11; COSMOlogic GmbH & Co.: KG, Leverkusen, Germany, 2010. (g) Ahlrichs, R.; Armbruster, M. K.; Bachorz, R. A.; Bär, M.; Baron, H.-P.; Bauernschmitt, R.; Bischoff, F. A.; Böcker, S.; Crawford, N.; Deglmann, P.; Sala, F. D.; Diedenhofen, M.; Ehrig, M.; Eichkorn, K.; Elliott, S.; Furche, F.; Glöß, A.; Haase, F.; Häser, M.; Hättig, C.; Hellweg, A.; Höfener, S.; Horn, H.; Huber, C.; Huniar, U.; Kattannek, M.; Klopper, W.; Köhn, A.; Kölmel, C.; Kollwitz, M.; May, K.; Nava, P.; Ochsenfeld, C.; Öhm, H.; Pabst, M.; Patzelt, H.; Rappoport, D.; Rubner, O.; Schäfer, A.; Schneider, U.; Sierka, M.; Tew, D. P.; Treutler, O.; Unterreiner, B.; von Arnim, M.; Weigend, F.; Weis, P.; Weiss, H.; Winter N. *TURBOMOLE*, v6.4; TURBOMOLE GmbH, 2012; see http://www.turbomole.com. (h) Tao, J. M.; Perdew, J. P.; Staroverov, V. N.; Scuseria, G. E. *Phys. Rev. Lett.* **2003**, *91*, 146401. (i) Zhao, Y.; Truhlar, D. G. *J. Phys. Chem. A* **2005**, *109*, 5656. (j) Schaefer, A.; Huber, C.; Ahlrichs, R. *J. Chem. Phys.* **1994**, *100*, 5829. (k) Weigend, F.; Häser, M.; Patzelt, H.; Ahlrichs, R. *Chem. Phys. Lett.* **1998**, *143*, 294.

(25) (a) Dewar, M. J. S. *Bull. Soc. Chim. Fr.* **1951**, *18*, C79. (b) Chatt, J.; Duncanson, L. A. *J. Chem. Soc.* **1953**, 2939. (c) Mingos, D. M. P. *J. Organomet. Chem.* **2001**, *635*, 1.

(26) See for a comparison: Ekkert, O.; Miera, G. G.; Wiegand, T.; Eckert, H.; Schirmer, B.; Petersen, J. L.; Daniliuc, C. G.; Fröhlich, R.; Grimme, S.; Kehr, G.; Erker, G. *Chem. Sci.* **2013**, *4*, 2657.

(27) Lim, M. D.; Lorkovic, I. M.; Ford, P. C. *Methods Enzymol.* **2005**, *396*, 3−17.

(28) Battino, R. *Fluid Phase Equilib.* **1984**, *15*, 231.

(29) Battino, R. *IUPAC: Solubility Data Series*; Pergamon Press: New York, 1981; Vol. *7*, p 452.

(30) Shaw, A. W.; Vosper, A. J. *J. Chem. Soc., Faraday Trans. 1* **1977**, *73*, 1239.